Waveforming Optimizations for Time-Reversal Cloud Radio Access Networks

Hang Ma, *Member, IEEE*, Beibei Wang, *Senior Member, IEEE*, Yan Chen, *Senior Member, IEEE*, and K. J. Ray Liu, *Fellow, IEEE*

***Abstract*— Due to the unique spatial and temporal focusing effects, time-reversal (TR) communication can be utilized in the cloud radio access network (C-RAN), where it creates "tunneling effects" such that the traffic load in the front-haul links can be alleviated in both downlink and uplink. Although the basic TR waveforms are simple to use, and they cannot provide the optimal performance in some cases. Since the C-RAN is usually expected to serve massive wireless devices, the severe inter-user interference will limit the performance of the system, especially in the high signal-to-noise ratio region where the interference power dominates the noise power. In this paper, we propose to optimize both downlink and uplink transmissions in the TR-based C-RAN so as to alleviate the interference. In the downlink transmission, an optimal content-aware waveform design is proposed, so that the baseband units (BBUs) are able to combine both the channel information and the content information to suppress the interference. In the uplink transmission, an optimal receiver design algorithm is proposed, such that the BBUs can detect the symbols transmitted by the terminal devices more accurately by leveraging the channel information. We study the bit error rate performance of the proposed algorithms based on extensive measurements of the wireless channel in a real-world environment. Numerical results demonstrate the significant performance improvement over the basic TR transmission techniques and the traditional waveform design techniques.**

***Index Terms*— Interference supression, broadband communication, least mean square methods, antenna arrays, MIMO systems, filtering.**

I. Introduction

CLOUD based radio access network (C-RAN) has been recently proposed [1]–[4] as a novel type of RAN architecture, where a pool of base band units (BBUs) are connected to the distributed remote radio heads (RRHs) via high bandwidth and low latency links. The BBUs are responsible for all the baseband processing through high performance computing. In this system, the spectral and energy efficiencies are improved by the centralized processing. Nevertheless, the limited front-haul link capacity is a bottleneck that hinders the system from fully achieving the benefits brought by concentrating the processing intelligence [5]. To tackle this challenge, current approaches include signal compression [6]–[8] and sparse beamforming [9], [10].

Time-reversal (TR) communication [11] is a new broadband wireless communication technique with unique spatial and temporal focusing effects in a rich-scattering environment. All the terminal devices (TDs) are naturally separated by their location-specific signatures in both downlink [12] and uplink [13]. Due to these nice features, Ma *et al.* [14] proposed to use the TR communications as the air interface for both the uplink and downlink of C-RAN. It was illustrated that the TR communications create "tunneling effects" in the front-haul links such that the baseband signals of multiple TDs can be efficiently combined and transmitted through the front-haul links to alleviate the traffic load.

In the TR based C-RAN proposed in [14], when the symbol duration is shorter than the delay spread of the multipath channel in high rate transmissions, the inter-symbol interference (ISI) may limit the performance of the system. Moreover, with network densification, e.g., in a C-RAN that needs to support a massive number of TDs, the severe inter-user interference (IUI) becomes the limiting factor that impairs both the spectral and energy efficiencies. Therefore, it is very important to design effective interference management schemes to improve the spectral and power efficiencies in TR based C-RAN.

In TR communication, algorithms for waveform design to maximize the sum achievable data rate in the downlink transmission were proposed in [15]. Yoon *et al.* [16] designed an interference alignment scheme aiming at managing the ISI in the single user case. In [13], a successive interference cancellation scheme was proposed to improve the performance in the uplink transmission. Nevertheless, these works only considered the case with a stand-alone single access point (AP), which is not applicable to the C-RAN architecture where multiple RRHs are expected to work together to deliver or receive information.

In the C-RAN literature, a lot of works have been done to utilize the computing power at the BBUs to optimize both the downlink and uplink transmissions. In [17], a joint precoding and compression scheme was proposed to alleviate the effect of interference and quantization noise so as to maximize the

Manuscript received June 24, 2016; revised December 10, 2016 and May 23, 2017; accepted September 8, 2017. Date of publication September 18, 2017; date of current version January 13, 2018. The associate editor coordinating the review of this paper and approving it for publication was L. Liu. *(Corresponding author: Hang Ma.)*

H. Ma was with the Department of Electrical and Computer Engineering, University of Maryland at College Park, College Park, MD 20742 USA, and also with Origin Wireless Communications Inc., College Park, MD 20742 USA. He is now with Google Inc., Mountain View, CA 94043 USA (e-mail: mahang2010@gmail.com).

B. Wang and K. J. R. Liu are with the Department of Electrical and Computer Engineering, University of Maryland at College Park, College Park, MD 20742 USA, and also with Origin Wireless Inc., College Park, MD 20742 USA (e-mail: bebewang@umd.edu; kjrliu@umd.edu).

Y. Chen was with the Department of Electrical and Computer Engineering, University of Maryland at College Park, College Park, MD 20742 USA and also with Origin Wireless Communications Inc., College Park, MD 20742 USA. He is now with the School of Electronic Engineering, University of Electronic Science and Technology of China, Chengdu 610051, China (e-mail: eecyan@uestc.edu.cn).

Color versions of one or more of the figures in this paper are available online at http://ieeexplore.ieee.org.

Digital Object Identifier 10.1109/TCOMM.2017.2753253

weighted sum rate in the downlink transmission. In order to comply with the limited front-haul link capacity of each RRH, a sparse beamforming and clustering technique was proposed in [9]. Zhou and Yu [6] authors proposed a joint beamforming and compression scheme for the uplink transmission in C-RAN. Researchers also investigated the power consumption issues of C-RAN in [18] and [19]. However, to the best of our knowledge, no optimization technique is available for the "asymmetric" architecture of the TR based C-RAN [14], i.e., much of the complexity is moved to the BBU side while the TDs can be of very low complexity in both downlink and uplink transmissions. In the downlink transmission of a TR based system, the TDs detect the transmitted signal by single-tap detection, while in the uplink they directly transmit the symbols after simple amplification.

In this work, we aim to optimize the downlink and uplink waveforms beyond the basic TR waveforms used in [14] so that the transmissions become more reliable and efficient. In the downlink, since the instantaneous channel impulse responses (CIRs) as well as the intended symbols of all the TDs are available at the BBUs, we propose algorithms that combine these information to optimally determine the power allocation and transmitting waveforms to minimize the mean square error (MSE) of the signal received by the TDs. In the uplink, since only the CIRs of all the TDs are available at the BBUs, we propose to utilize this information to optimize the receiver design as well as the transmitting power of all the TDs. All the proposed algorithms are guaranteed to converge. To illustrate the effectiveness of the proposed schemes, we conduct experiments to measure the multipath channel information in a real-world environment, based on which we show that the proposed schemes can significantly reduce the bit error rate (BER) of both downlink and uplink transmissions compared with using the basic TR waveforms. As a result, the number of re-transmissions caused by transmission errors are reduced, which further alleviates the traffic load in the front-haul links. Moreover, since all these optimizations are performed in the BBUs, the asymmetric architecture of the TR based C-RAN is preserved, and the performance is improved without any change at the TD side.

The rest of the paper is organized as follows: in section II, both downlink and uplink waveform optimization problems are formulated; the downlink waveform is optimized in section III; the uplink detector and power control are optimized in section IV; numerical results are shown in section V and section VI concludes this paper.

II. System Models and Problem Formulations

In the indoor broadband wireless communication, the signal suffers from the multipath effect caused by the reflections of the indoor environment. Instead of trying to avoid the multipath effect, TR based communication utilizes all the multipaths to act like a matched filter to achieve spatial and temporal focusing effects. In Fig. 1, we show the typical process of a TR communication. For example, transceiver B tries to transmit some information to transceiver A. Prior to the transmission, the transceiver A has to send out a delta-like pilot pulse which propagates to transceiver B through a

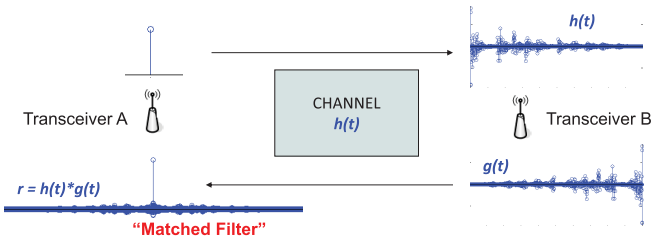

Fig. 1. The schematic diagram of the time reversal system.

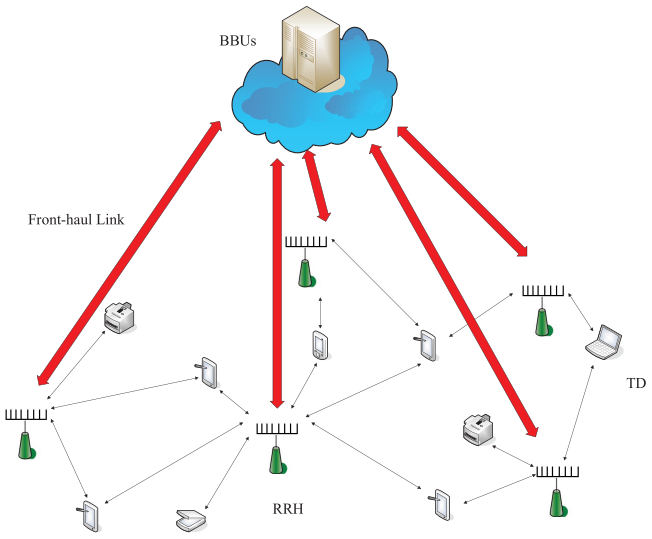

Fig. 2. The System Model.

multi-path channel, and transceiver B keeps a record of the received waveform h. Then, the transceiver B time reverses the received waveform, and use the normalized time-reversed conjugate signals as a basic waveform g, i.e.,

$$g[k] = \frac{h^*[L-1-k]}{\sqrt{\sum_{l=0}^{L-1} \|h[l]\|^2}} \tag{1}$$

where $L = \frac{\delta_T}{TS}$ is the channel length, TS is the sampling period of the transceivers such that $\frac{1}{TS}$ equals to the bandwidth B used and δ_T is the delay spread of the channel [20]. Due to the channel reciprocity, when transceiver B transmits g using the same band which transceiver A uses for the pilot pulse, the multi-path channel forms a natural matched filter by performing $h * g$, and hence a peak is expected at the receiver.

In the time-reversal (TR) based cloud radio access network (C-RAN) [14] shown in Fig. 2, the terminal devices (TDs) periodically send known sequences of waveforms to the remote radio heads (RRHs) in the channel probing phase. The RRHs transmit the received baseband signal to the baseband units (BBUs), which then detect the channel impulse response (CIR) using the received signal. According to section II.B of [14], the channel probing overhead is less than 0.1% for a typical TD moving with walking speed, and the system-wide overhead is approximately $N * 0.1\%$ where N is the total number of TDs that require frequent channel information update. The channel probing time is independent of the number of RRHs or number of antennas per RRH. In this system, the downlink and uplink transmissions work

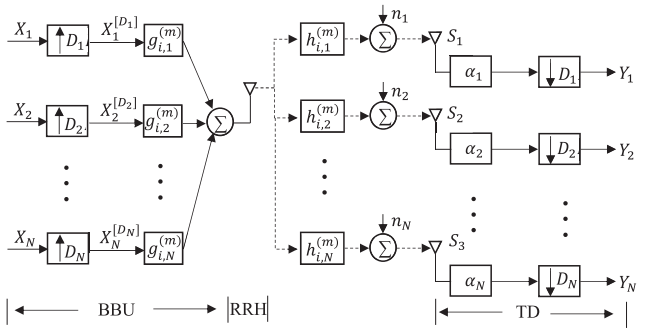

Fig. 3. The Downlink Transmission Diagram.

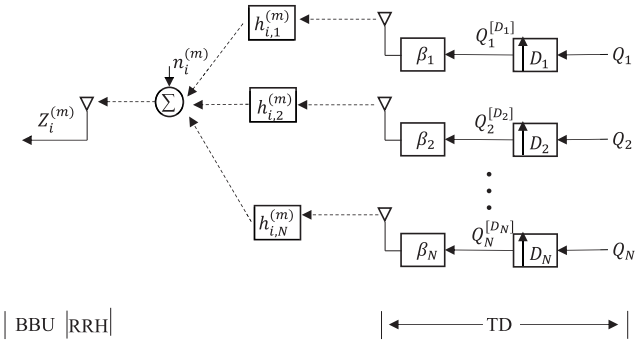

Fig. 4. The Uplink Transmission Diagram.

by time division duplexing (TDD) such that the CIR can be shared. The CIR is considered as the transmitting waveform of the corresponding TD, and used by the BBUs for the downlink and uplink data transmissions. In the downlink data transmission shown in Fig. 3, the BBUs simply use the time-reversed version of the CIR as the symbol waveform to transmit the data symbols. After receiving the signal, the TD detects the transmitted symbols by looking at one sample of the received signal for each symbol. As a consequence, the complexity at the TD side can be very low while most of the computational burden is shifted to the BBUs. In the uplink data transmission shown in Fig. 4, the TDs amplify and transmit the symbols to the RRHs through the multipath channels without any other complicated processing. The RRHs transmit the received signal through the front-haul links to the BBUs and the BBUs then convolve the received signal with the time-reversed version of the CIR of corresponding TDs to detect the symbols transmitted by the TDs.

Although using basic TR waveform is simple and straightforward, it cannot achieve the optimal performance, especially in the dense network where the inter-user interference (IUI) becomes the limiting factor. In this work, we focus on the waveform design problem to optimize both downlink and uplink data transmissions. The downlink and uplink waveform design problem will be formulated separately in the following.

A. Downlink Problem Formulation

We will first analyze the case that a single RRH serves multiple TDs. Without loss of generality, we assume that each RRH is equipped with MT antennas and each TD is equipped with 1 antenna. Let $h_{i,k}^{(m)}$ denote the multipath channel between the m-th antenna of the i-th RRH and the k-th TD, which is a column vector of length L with L being the maximum channel length of all the N TDs. Let column vectors X_k and $g_{i,k}^{(m)}$ denote the information symbols and the transmit waveform for user k at the m-th antenna of RRH i. $g_{i,k}^{(m)}$ can be basic TR waveform or more advanced waveform. The length of $g_{i,k}^{(m)}$ is also L. In this work, we consider the frame-based transmission and reception schemes. The frame of symbols for user k is denoted by $X_k = [x_{k,1}, x_{k,2}, \cdots x_{k,F_k}]^T$ where F_k is the frame length of TD k. As shown Fig. 3, at the m-th antenna of RRH i, the X_k will be first upsampled by the backoff factor D_k for inter-symbol interference (ISI) alleviation. The upsampled symbol frame is denoted as $X_k^{[D_k]}$. After that, a blank sub-frame is appended to the end of the up-sampled signal to prevent the interference between frames. The length of the sub-frame is no less than L taps. Then, the entire frame is convolved with the downlink transmission signature $g_{i,k}^{(m)}$, after which the convoluted signal for all the TDs are summed up together and transmitted over the air to multiple TDs simultaneously.

The signal received at TD k can be represented as

$$S_k = \sum_{m=1}^{MT} h_{i,k}^{(m)} * (\sum_{\upsilon=1}^{N} g_{i,\upsilon}^{(m)} * X_{\upsilon}^{[D_\upsilon]}) + n_k \tag{2}$$

where n_k is the noise vector with appropriate length. Without loss of generality, we assume the noise power $E[\|n_k[j]\|^2] = \sigma^2, \forall k, j$.

The k-th TD will first amplify the S_k with α_k and then downsample it with the backoff factor D_k, obtaining the receiced sequence Y_k, based on which it will try to detect X_k. The received sequence Y_k can be represented as

$$Y_k = \alpha_k M_k \sum_{m=1}^{MT} h_{i,k}^{(m)} * (\sum_{\upsilon=1}^{N} g_{i,\upsilon}^{(m)} * X_{\upsilon}^{[D_\upsilon]}) + \alpha_k M_k n_k \tag{3}$$

where M_k is a masking matrix for TD k since only the sampled taps of the received signal are considered. More specifically,

$$M_k = [e_L; \quad e_{L+D_k}; \quad \cdots \quad e_{L+(F_k-1)D_k}], \tag{4}$$

where e_i denotes the i-th row of the $(2L - 1 + (F_k - 1)D_k) \times (2L - 1 + (F_k - 1)D_k)$ identity matrix.

We define $H_{i,k}^{(m)}$ as the Toeplitz matrix of size $(2L-1) \times L$ with the first column being $[(h_{i,k}^{(m)})^T \ \ \mathbf{0}_{1\times\ (L-1)}]^T$, then Y_k can be further written as

$$Y_k = \alpha_k \cdot \tilde{B}_{i,k} g_i + \alpha_k \cdot M_k n_k, \tag{5}$$

where

$$g_i = \begin{pmatrix} g_{i,1} \\ g_{i,2} \\ \vdots \\ g_{i,N} \end{pmatrix} \tag{6}$$

is the aggregation of all the downlink transmission signature $g_{i,k}$'s. The $g_{i,k}$ is defined as

$$g_{i,k} = \begin{pmatrix} g_{i,k}^{(1)} \\ g_{i,k}^{(2)} \\ \vdots \\ g_{i,k}^{(MT)} \end{pmatrix}, \tag{7}$$

which is the the aggregation of the downlink transmission signature $g_{i,k}^{(m)}$'s between all the antennas of RRH i and TD k. The $\tilde{B}_{i,k}$ is the equivalent channel matrix combining both the channel information $h_{i,k}^{(m)}$'s and content information X_k's. More specifically,

$$\tilde{B}_{i,k} = M_k[\tilde{B}_{i,k}^{(1)} \quad \tilde{B}_{i,k}^{(2)} \quad \cdots \quad \tilde{B}_{i,k}^{(N)}], \tag{8}$$

where

$$\tilde{B}_{i,k}^{(r)} = [\underset{F_k}{\tilde{B}_{i,k}^{(r),(1)}} \quad \cdots \quad \tilde{B}_{i,k}^{(r),(MT)}], \tag{9}$$

$$\tilde{B}_{i,k}^{(r),(m)} = \sum_{j=1} x_{r,j} \cdot H_{i,k}^{(m),(j)}, \tag{10}$$

with $x_{r,j}$ being the j-th tap of X_r and

$$H_{i,k}^{(m),(j)} = \begin{pmatrix} \mathbf{0}_{(j-1)D_k \times L} \\ H_{i,k}^{(m)} \\ \mathbf{0}_{(F_k-j)D_k \times L} \end{pmatrix} \tag{11}$$

is the augmented matrix of $H_{i,k}^{(m)}$ with size $(2L - 1 + (F_k - 1)D_k) \times L$.

In the TR communication system, due to the asymmetric architecture [12], [13], all the computation complexity are migrated to the BBUs and the TDs have low complexity. In other words, the TDs are unable to perform sophisticated signal processing to detect the transmitted symbols. Due to this constraint, we aim to make the received signal Y_k close to X_k so that TD k could directly get the transmitted information based on the received signal.

To achieve this, some sophisticated processing are needed at the BBU side. It can be seen in (5) that we combine the channel information $h_{i,k}$'s and the content information X_k's in the matrix $\tilde{B}_{i,k}$, which are readily available at the BBUs, and the BBUs can instantaneously compute the $\tilde{B}_{i,k}$'s and utilize them to optimize the downlink data transmission. Since all the TDs simultaneously work at the same spectrum, each TD suffers from the inter-symbol interference (ISI) and the inter-user interference (IUI), which are significantly affected by the design of g_i. We aim to find the optimal g_i and $\alpha = [\alpha_1, \alpha_2, \quad \cdots \quad \alpha_N]$ to minimize the mean square error (MSE) of the received signal without violating the transmitting power constraints. More specifically, the optimization problem becomes

$$\begin{aligned} &\min_{\alpha, g_i} \sum_{k=1}^{N} E[\|Y_k - X_k\|^2] \\ &\text{s.t. } g_i' g_i \le P_{max}^{(dl)}, \end{aligned} \tag{12}$$

where $P_{max}^{(dl)}$ is the maximum transmitting power allowed for each RRH in the downlink transmission. Note that by (7) the number of antennas of RRH i affects the dimension of the vector g_i. The more antennas available, the higher degree of freedom can be used for the optimization.

B. Uplink Problem Formulation

In the uplink of the TR based C-RAN system, All the TDs simultaneously transmit the information through the RRHs to the BBUs. The BBUs collect the information received by all the RRHs and then detect the transmitted symbols by processing the received signal. We will first analyze the case that a single RRH serves multiple TDs. Similar to the downlink case, the uplink will also be using the frame based transmission. The frame of symbols of TD k is denoted by the column vector $Q_k = [q_{k,1}, q_{k,2}, \cdots q_{k,T_k}]^T$ where T_k is the frame length of TD k. As shown in Fig. 4, at TD k, the Q_k will be first upsampled by the backoff factor D_k for ISI alleviation. After that, a blank sub-frame is appended to the end of the up-sampled signal to prevent the interference between frames. The length of the sub-frame is no less than L taps. Then, the entire frame is amplified element-wisely by the elements of the column vector $\beta_k = [\beta_{k,1}, \beta_{k,2}, \cdots, \beta_{k,T_k}]$ and then transmitted over the air to each antenna at RRH i, i.e., the symbol $q_{k,j}$ is amplified by $\beta_{k,j}$. In Fig. 4, it shows the signal received at the m-th antenna of RRH i. The signal received at the RRH i is the aggregation of the signals from the MT antennas, which is

$$Z_i = \begin{pmatrix} Z_i^{(1)} \\ Z_i^{(2)} \\ \vdots \\ Z_i^{(MT)} \end{pmatrix}. \tag{13}$$

The signal received at the m-th antenna can be represented as

$$Z_i^{(m)} = R_i^{(m)} \beta Q + n_i^{(m)}, \tag{14}$$

where

$$Q = \begin{pmatrix} Q_1 \\ Q_2 \\ \vdots \\ Q_N \end{pmatrix} \tag{15}$$

is the aggregation of the frames of all the TDs,

$$R_i^{(m)} = \begin{pmatrix} R_{i,1}^{(m)} & R_{i,2}^{(m)} & \cdots & R_{i,N}^{(m)} \end{pmatrix}, \tag{16}$$

and β is a diagonal matrix with the diagonal elements being $\beta_{1,1}, \cdots \beta_{1,T_1}, \beta_{2,1}, \cdots \beta_{2,T_2}, \cdots, \beta_{N,1}, \cdots \beta_{N,T_N}$. $R_{i,j}^{(m)}$ is the Toeplitz matrix of size $(D_j \cdot (T_j - 1) + L) \times T_j$ with the j-th column being $[\mathbf{0}_{(j-1)*D_j}; (h_{i,j}^{(m)})^T; \mathbf{0}_{(T_j-j)\times D_j}]$.

The aggregate received signal Z_i can be re-written as

$$Z_i = \begin{pmatrix} R_i^{(1)} \\ R_i^{(2)} \\ \vdots \\ R_i^{(MT)} \end{pmatrix} \beta Q + \begin{pmatrix} n_i^{(1)} \\ n_i^{(2)} \\ \vdots \\ n_i^{(MT)} \end{pmatrix}, \tag{17}$$

It can be seen that the channel information $h_{i,k}^{(m)}$'s are combined in $R_i^{(m)}$, which are readily available at the BBUs in

the uplink. Moreover, the BBUs are equipped with all the computation power so that they have the ability to process the received signal in sophisticated ways to extract the information transmitted by the TDs. In this work, we aim to design the linear minimum mean square error (LMMSE) detector W_i to detect the symbols transmitted by the TDs. Moreover, the BBUs need also determine the power control factor $\beta_{k,j}$'s in order to avoid the strong-weak effect. The problem can be formulated as

$$\begin{aligned} &\min_{\beta, W_i} \ E[\|W_i Z_i - Q\|^2] \\ &\text{s.t. } \beta_{k,j}^2 E[\|q_{k,j}\|^2] \le P_{max}^{(ul)}, \quad \forall k, j, \end{aligned} \tag{18}$$

where $P_{max}^{(ul)}$ is the maximum transmitting power allowed for each TD in the uplink transmission. Note that by (17), the number of antennas at RRH i affects the dimensions of Z_i and W_i. The more antennas available, the higher degree of freedom can be utilized in the optimization.

III. Downlink Waveform Design

In this section, we solve the problem (12) formulated in section II to optimize the downlink data transmission. We will start with the single RRH multiple TD case. Since the problem in (12) is a non-convex problem, we propose to use iterative algorithms to solve it. Through designing the algorithm, we find that under a special single TD case, a closed form optimal waveform design can be derived. Eventually, we extend the problem to the coordinated waveform design such that multiple RRHs can work together to focus the signal at the intended locations.

A. Single RRH Waveform Design and Power Allocation

In this subsection, we will analyze the waveform design problem in the case that a single RRH serves multiple TDs. The MSE of TD k can be expressed as

$$\begin{aligned} MSE_k &= E[\|\alpha_k \tilde{B}_{i,k} g_i + \alpha_k M_k n_k - X_k\|^2] \\ &= \|\alpha_k\|^2 g_i' \tilde{B}_{i,k}' \tilde{B}_{i,k} g_i - \alpha_k' g_i' \tilde{B}_{i,k}' X_k - \alpha_k X_k' \tilde{B}_{i,k} g_i \\ &\quad + \|\alpha_k\|^2 F_k \sigma^2 + X_k' X_k \end{aligned} \tag{19}$$

The total MSE can be represented as

$$\begin{aligned} \sum_{k=1}^N MSE_k = g_i'(\sum_{k=1}^N \|\alpha_k\|^2 \tilde{B}_{i,k}' \tilde{B}_{i,k}) g_i - g_i'(\sum_{k=1}^N \alpha_k' \tilde{B}_{i,k}' X_k) \\ -(\sum_{k=1}^N \alpha_k X_k' \tilde{B}_{i,k}) g_i + \sum_{k=1}^N X_k' X_k + \sum_{k=1}^N \|\alpha_k\|^2 F_k \sigma^2 \end{aligned} \tag{20}$$

The problem in (12) becomes

$$\begin{aligned} \min_{\alpha, g_i} \ & g_i'(\sum_{k=1}^N \|\alpha_k\|^2 \tilde{B}_{i,k}' \tilde{B}_{i,k}) g_i - g_i'(\sum_{k=1}^N \alpha_k' \tilde{B}_{i,k}' X_k) \\ & - (\sum_{k=1}^N \alpha_k X_k' \tilde{B}_{i,k}) g_i + \sum_{k=1}^N \|\alpha_k\|^2 F_k \sigma^2 \\ \text{s.t. } & g_i' g_i \le P_{max}^{(dl)}, \end{aligned}$$

which is a non-convex optimization problem. Since each TD's optimal $g_{i,k}$ and α_k depend on those of other TDs, the closed form global optimal solution is difficult to find. In the following, we provide two algorithms that are guaranteed to converge to a local optimal point.

1) Alternating Optimization Algorithm: In this subsection, we will introduce the alternating optimization algorithm, where we alternatively optimize one of g_i and α given the other.

The Lagrangian of the problem in (21) can be written as

$$\begin{aligned} L(\alpha, g_i, \lambda) = g_i'(\sum_{k=1}^N \|\alpha_k\|^2 \tilde{B}_{i,k}' \tilde{B}_{i,k}) g_i - g_i'(\sum_{k=1}^N \alpha_k' \tilde{B}_{i,k}' X_k) \\ -(\sum_{k=1}^N \alpha_k X_k' \tilde{B}_{i,k}) g_i + \sum_{k=1}^N \|\alpha_k\|^2 F_k \sigma^2 \\ + \lambda(g_i' g_i - P_{max}^{(dl)}). \end{aligned} \tag{21}$$

Given g_i, optimizing α is an unconstrained optimization problem, which can be solved by

$$\frac{\partial L}{\partial \alpha_k} = 0 \Rightarrow \alpha_k = (F_k \sigma^2 + g_i' \tilde{B}_{i,k}' \tilde{B}_{i,k} g_i)^{-1} g_i' \tilde{B}_{i,k}' X_k. \tag{22}$$

Next, we will derive how to optimize g_i given α. We have

$$\frac{\partial L}{\partial g_i} = 0 \Rightarrow g_i'(\sum_{k=1}^N \|\alpha_k\|^2 \tilde{B}_{i,k}' \tilde{B}_{i,k}) - \sum_{k=1}^N \alpha_k X_k' \tilde{B}_{i,k} + \lambda g_i' = 0. \tag{23}$$

By solving (22) and (23), we can have

$$\lambda = \frac{\sum_{k=1}^N \|\alpha_k\|^2 F_k \sigma^2}{P_{max}^{(dl)}}. \tag{24}$$

Substituting (24) into (23), we can have

$$\begin{aligned} g_i = (\sum_{k=1}^N \|\alpha_k\|^2 \tilde{B}_{i,k}' \tilde{B}_{i,k} \\ + \frac{\sum_{k=1}^N \|\alpha_k\|^2 F_k \sigma^2}{P_{max}^{(dl)}} \mathbf{I})^{-1} (\sum_{k=1}^N \alpha_k' \tilde{B}_{i,k}' X_k). \end{aligned} \tag{25}$$

The alternating optimization algorithm can be summarized in Algorithm 1.

Algorithm 1 Alternating Optimization Algorithm

1 Initialize $\alpha_k = 1, \ \forall k$
2 **loop:**
3 Calculate g_i according to (25)
4 Calculate α_k's according to (22)
5 **until** g_i and α_k's converge or the maximum number of iterations is reached

In the alternating optimization algorithm, the MSE is non-increasing each time we update α_k or g_i. As a result, the MSE is non-increasing as the iteration goes on. Since the

MSE in (21) is lower bounded, the proposed algorithm is guaranteed to converge.

Although the problem in (21) is non-convex, an interesting observation is that when there is only one TD, by solving the Lagrangian, we find that the necessary conditions lead to a unique solution, which is the optimal solution for (21). Specifically, from (22) we have

$$\|\alpha_k\|^2 g_i' \tilde{B}_{i,k}' \tilde{B}_{i,k} g_i + \|\alpha_k\|^2 F_k \sigma^2 = \alpha_k X_k' \tilde{B}_{i,k} g_i. \quad (26)$$

From (23) we have

$$\|\alpha_k\|^2 g_i' \tilde{B}_{i,k}' \tilde{B}_{i,k} g_i + \lambda g_i' g_i = \alpha_k X_k' \tilde{B}_{i,k} g_i. \quad (27)$$

By comparing (26) and (27), we can have $\|\alpha_k\|^2 F_k \sigma^2 = \lambda g_i' g_i$. Obviously, $\lambda = 0 \Rightarrow \alpha_k = 0$, which is not an optimal solution. If $\lambda \neq 0$, we have

$$g_i' g_i = P_{max}^{(dl)} \quad (28)$$

by complementary slackness [21]. Therefore, $\lambda = \frac{\|\alpha_k\|^2 F_k \sigma^2}{P_{max}^{(dl)}}$. Substituting the solution of λ into (23), we can obtain

$$g_i = \alpha_k' (\|\alpha_k\|^2 \tilde{B}_{i,k}' \tilde{B}_{i,k} + \frac{\|\alpha_k\|^2 F_k \sigma^2}{P_{max}^{(dl)}} \mathbf{I})^{-1} \tilde{B}_{i,k}' X_k, \quad (29)$$

where $\mathbf{I}$ is an identity matrix. By substituting (29) into (28), we have

$$\|\alpha_k\|^2 = \frac{X_k' \tilde{B}_{i,k} (\tilde{B}_{i,k}' \tilde{B}_{i,k} + \frac{F_k \sigma^2}{P_{max}} \mathbf{I}) \tilde{B}_{i,k}' X_k}{P_{max}}. \quad (30)$$

Obviously, the solution to (30) is not unique. In the single TD case, as can be seen from (25) and (29) , for each α_k satisfying (30), the MSEs are the same by (20) since the corresponding g_i compensates the phase. Therefore, without loss of generality, we choose the real valued solution of α_k

$$\alpha_k = \sqrt{\frac{X_k' \tilde{B}_{i,k} (\tilde{B}_{i,k}' \tilde{B}_{i,k} + \frac{F_k \sigma^2}{P_{max}^{(dl)}} \mathbf{I})^{-2} \tilde{B}_{i,k}' X_k}{P_{max}^{(dl)}}}. \quad (31)$$

Substituting (31) into (29), we can obtain the optimal waveform for the single user. The resulting MSE in the single user case can be expressed as

$$MSE^{SU} = X_k' X_k - X_k' \tilde{B}_{i,k} (\tilde{B}_{i,k}' \tilde{B}_{i,k} + \frac{F_k \sigma^2}{P_{max}^{(dl)}} \mathbf{I})^{-1} \tilde{B}_{i,k}' X_k. \quad (32)$$

We observe that in this problem, the optimal solution satisfies $g_i' g_i = P_{max}^{(dl)}$. In other words, when only one single TD is served by the RRH, the RRH always uses full power for the downlink transmission. This conclusion can be verified in another way. If there are certain g_i and α_k such that $g_i' g_i < P_{max}^{(dl)}$, then we can always scale up g_i until it reaches $P_{max}^{(dl)}$, and scale down α_k accordingly to keep the first term in (5) the same while reducing the power of the second term, which is the power of the noise. As a result, the impairment caused by noise is alleviated and the MSE can be reduced.

2) Gradient Algorithm: In addition to the alternating optimization algorithm, we also propose another algorithm to find the optimal waveform.

From (22), we are able to calculate the optimal α_k given g_i. By plugging (22) into (19), the MSE of the k-th TD can be expressed as

$$MSE_k = X_k' X_k - \frac{g_i' \tilde{B}_{i,k}' X_k X_k' \tilde{B}_{i,k} g_i}{g_i' \tilde{B}_{i,k}' \tilde{B}_{i,k} g_i + F_k \sigma^2}. \quad (33)$$

The total MSE of all the TDs can be represented as

$$\sum_{k=1}^{N} MSE_k = \sum_{k=1}^{N} (X_k' X_k - \frac{g_i' \tilde{B}_{i,k}' X_k X_k' \tilde{B}_{i,k} g_i}{g_i' \tilde{B}_{i,k}' \tilde{B}_{i,k} g_i + F_k \sigma^2}). \quad (34)$$

The gradient can be calculated as

$$\begin{aligned} \nabla g_i &\triangleq \frac{\partial}{\partial g_i} (\sum_{k=1}^{N} MSE_k) \\ &= \sum_{k=1}^{N} [\frac{2 \tilde{B}_{i,k}' \tilde{B}_{i,k} g_i (g_i' \tilde{B}_{i,k}' X_k X_k' \tilde{B}_{i,k} g_i)}{(g_i' \tilde{B}_{i,k}' \tilde{B}_{i,k} g_i + F_k \sigma^2)^2} \\ &\quad - \frac{2 \tilde{B}_{i,k}' X_k X_k' \tilde{B}_{i,k} g_i}{g_i' \tilde{B}_{i,k}' \tilde{B}_{i,k} g_i + F_k \sigma^2}]. \end{aligned} \quad (35)$$

Once the gradient is calculated, we use it to update the waveform in order to minimize the MSE. Moreover, we project it to the constraint set $g_i' g_i = P_{max}^{(dl)}$ by normalization to comply with the transmitting power constraint. Specifically,

$$g_i^{new} = g_i - \delta_n \cdot \nabla g_i \quad (36)$$

$$g_i^{new,p} = \frac{\sqrt{P_{max}^{(dl)}}}{\|g_i^{new}\|} \cdot g_i^{new}, \quad (37)$$

where the first equation is to determine the shape of the new waveform by line search. We choose the step size for the n-th iteration in line search as $\delta_n = \frac{1}{n}$ for its good convergence behavior [21]. The second equation is to project the waveform into the space satisfying the transmitting power constraint. The gradient optimization algorithm can be summarized in Algorithm 2.

Algorithm 2 Gradient Optimization Algorithm

```
Initialize g_i as the basic TR waveform
loop:
    Calculate ∇g according to (35)
    Set n = 1
    Update g_i^{new,p} according to (36) and (37)
    if MSE_new < MSE_current
        g_i = g_i^{new,p}
    else
        n = n + 1, go to step 5
until g_i and α_k's converge or the maximum number
    of iterations is reached
```

In this algorithm, g_i is updated in step 7 only when the MSE is reduced by the update. Therefore, the MSE is non-increasing in this algorithm. Since the MSE is lower bounded, the gradient algorithm is guaranteed to converge.

B. Extension to Multi-RRH Joint Waveform Design and Power Allocation

In this subsection, we will extend the gradient algorithm to the multiple RRH case so that multiple RRHs are able to jointly determine the waveform for the downlink transmission so as to better focus the signal at the intended TDs.

First, we extend the problem in (12) to the multiple RRH case. When multiple RRHs work together to serve the TDs distributed in the area, each TD simultaneously receives and combines the signal transmitted by all the serving RRHs. Suppose there are totally M RRHs serving N TDs in the area. The signal received by TD k can be represented as

$$\begin{aligned} Y_k &= \alpha_k \sum_{i=1}^{M} \tilde{B}_{i,k} g_i + \alpha_k \cdot M_k n_k \\ &= \alpha_k \cdot \tilde{B}_k g + \alpha_k \cdot M_k n_k, \end{aligned} \tag{38}$$

where

$$g = \begin{pmatrix} g_1 \\ g_2 \\ \vdots \\ g_M \end{pmatrix} \tag{39}$$

is the aggregation of all the downlink transmission signature g_i's of the RRH i, and

$$\tilde{B}_k = [\tilde{B}_{1,k} \quad \tilde{B}_{2,k} \quad \cdots \quad \tilde{B}_{M,k}]. \tag{40}$$

Since the transmitting power at each of the RRHs cannot exceed $P_{max}^{(dl)}$, the problem in (12) becomes

$$\begin{aligned} \min_{\alpha,g} \; & g'(\sum_{k=1}^{N} \|\alpha_k\|^2 \tilde{B}'_{i,k} \tilde{B}_k) g - g'(\sum_{k=1}^{N} \alpha'_k \tilde{B}'_k X_k) \\ & -(\sum_{k=1}^{N} \alpha_k X'_k \tilde{B}_k) g + \sum_{k=1}^{N} \|\alpha_k\|^2 F_k \sigma^2 \\ \text{s.t. } & g'_i g_i \le P_{max}^{(dl)}, \; \forall i. \end{aligned} \tag{41}$$

The gradient optimization algorithm proposed earlier can be modified to work in the multiple RRH case. Since each single RRH has only limited transmitting power, the projection in (37) is modified by normalizing the maximum transmitting power of all the RRHs to $P_{max}^{(dl)}$, while the transmitting power of all the other RRHs are scaled down accordingly. Specifically, the projection step is

$$g^{new,p} = \frac{\sqrt{P_{max}^{(dl)}}}{\max_i \|g_i\|} \cdot g_{new}. \tag{42}$$

By solving problem (41), all the RRHs work together to determine the optimal g without violating the transmitting power constraint at each of the RRHs. As a result, the transmitted signal are better focused at the intended receivers with little leakage to the surroundings. It will be shown later in the numerical results that, compared with the single RRH case, multiple RRHs not only bring in extra power, but also additional degree of freedom so that the signal can be focused at the intended locations more sharply.

IV. Uplink Joint Power Control and Detector Design

In this section, we try to solve the problem (18) formulated in section II. We will first analyze the single RRH case where RRH i determines the transmitting power of all the TDs and then processes the received signal to extract the uplink information. Then we extend it to the multiple RRH case where the BBUs can leverage the signal collected by more than one RRHs.

A. Single RRH Power Control and Detector Design

Suppose the RRH i collects the uplink signal transmitted by N TDs and forward it to the BBUs for further processing. The MSE in (18) can be written as

$$\begin{aligned} E[\|W_i Z_i - Q\|^2] &= E[\|W_i R_i \beta Q + W_i n_i - Q\|^2] \\ &= trace[(\beta' R'_i \Sigma_e^{-1} R_i \beta + \Sigma_q^{-1})^{-1}]. \end{aligned} \tag{43}$$

Before diving into solving the optimization problem, it's worthwhile explaining the differences in problems formulations for downlink and uplink. In (43), the content symbols Q are averaged out and only the power Σ_q is taken into consideration. On the other hand, the content information X are preserved in (19) and taken into the optimization problem. The reason is that since all the waveformings are performed in the BBUs side, the content information is available in the downlink but not in the uplink. Therefore, the content-aware waveforming is only possible in the downlink. In this work, we use the LMMSE detector to detect Q. In [22], the LMMSE detector can be written as

$$W_i = \Sigma_q \beta' R'_i (R_i \beta \Sigma_q \beta' R'_i + \Sigma_e)^{-1}, \tag{44}$$

where

$$\begin{aligned} \Sigma_q &= E[QQ'] \\ \Sigma_e &= E[n_i n'_i]. \end{aligned} \tag{45}$$

It can be seen that if β is available, the LMMSE detector can be determined. The MSE can be written as

$$MSE^{(ul)} = trace[(\beta' R'_i \Sigma_e^{-1} R_i \beta + \Sigma_q^{-1})^{-1}], \tag{46}$$

which is affected by β. Moreover, β is also limited by the transmitting power constraints of the TDs. Since the R_i, Σ_q and Σ_e are available at the BBUs, the BBUs are able to optimize over β in order to further minimize the MSE, and signal them to the TDs through the control/feedback links. The problem becomes

$$\begin{aligned} \min_{\beta} \; & trace[(\beta' R'_i \Sigma_e^{-1} R_i \beta + \Sigma_q^{-1})^{-1}] \\ \text{s.t. } & \beta_{k,j} \le \sqrt{\frac{P_{max}^{(ul)}}{E[\|q_{k,j}\|^2]}}, \quad \forall k, j, \end{aligned} \tag{47}$$

Fig. 5. The TR Radio Prototype.

which is a non-convex problem. Since the global optimal solution is hard to find, in the following, we use a gradient algorithm to find the optimal β to minimize the MSE while satisfying the transmission power constraint of each TD.

Let $A \triangleq \Sigma_e^{-\frac{1}{2}} R_i$. Note that β is a diagonal matrix. We calculate the gradient of the $MSE^{(ul)}$ with respect to each diagonal element of β. In [23], we have

$$\frac{\partial MSE^{(ul)}}{\partial \beta(s,s)} \triangleq \nabla\beta(s,s) = -trace[(\beta' A' A\beta + \Sigma_q)^{-2}(\psi_s' A' A\beta + \beta' A' A\psi_s)], \tag{48}$$

where ψ_s is a matrix the same size with β. All elements in ψ_s are zeros except that $\psi_s(s,s) = 1$.

The gradient of $MSE^{(ul)}$ with respect to β can be calculated as

$$\frac{\partial MSE^{(ul)}}{\partial \beta} \triangleq \nabla\beta = \begin{pmatrix} \nabla\beta(1,1) & 0 & \cdots & 0 \\ 0 & \nabla\beta(2,2) & \ddots & 0 \\ \vdots & \ddots & \ddots & \vdots \\ 0 & \cdots & 0 & \nabla\beta(U,U) \end{pmatrix}, \tag{49}$$

where $\nabla\beta$ is the diagonal matrix the same size with β, and the i-th item in the diagonal is $\nabla\beta(i,i)$. The total number of diagonal elements is $U = \sum_{i=1}^{N} T_i$.

After we obtain the gradient for each $\beta(s,s)$, we update each $\beta(s,s)$ by line search and projection similar to the downlink gradient algorithm. Specifically,

$$\beta^{new} = \beta - \delta_n \cdot \nabla\beta, \tag{50}$$

$$\beta^{proj} = \frac{\sqrt{P_{max}^{(ul)}}}{\max_s(\beta^{new}(s,s)\sqrt{\Sigma_q(s,s)})}\beta^{new}, \tag{51}$$

where we choose $\delta_n = \frac{1}{n}$. The algorithm can be summarized in Algorithm 3.

In this algorithm, β is updated in step 7 only when the MSE is reduced by the update. Therefore, the MSE is non-increasing in this algorithm. Since the MSE is lower bounded, the gradient algorithm is guaranteed to converge.

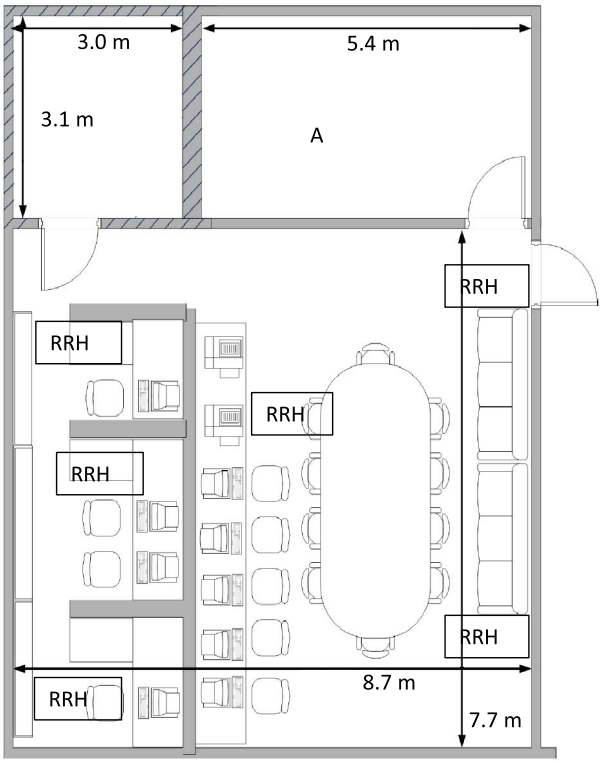

(a) The Floor Plan of The Testing Room

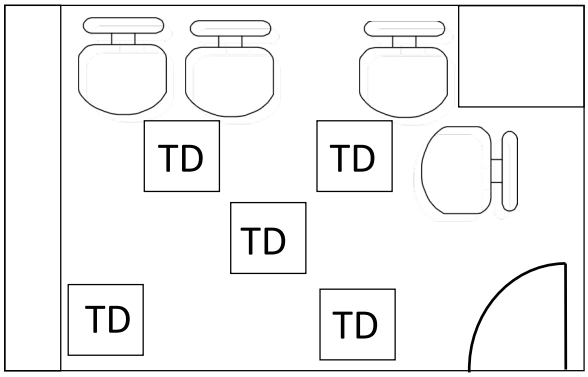

(b) Floor Plan of Room A

Fig. 6. The Floor Plan of the Testing Sites.

B. Extension to the Multiple RRH Joint Power Control and Detector Design

In the above, we proposed the joint LMMSE detector design and power control algorithm in the single RRH case so that the BBUs can determine the optimal transmitting power utilized by each TD and then use the baseband signal collected by RRH i to extract the information transmitted by all the TDs. In the C-RAN setting, usually more than one RRHs are available in a specific area. Compared to the single RRH case, extra RRHs can provide additional information about the signal transmitted by the TDs, which can be utilized to improve the accuracy in detecting the transmitted symbols.

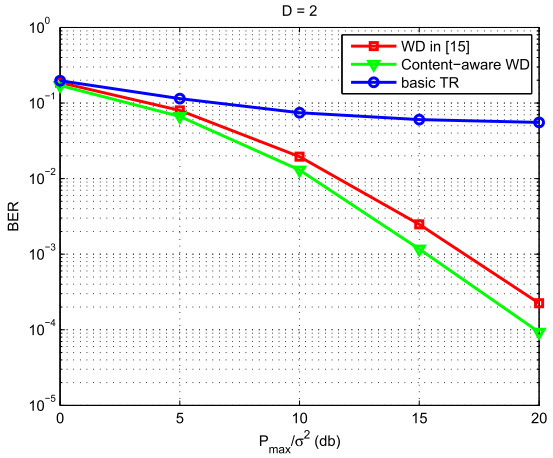

(a) The BER of the single RRH single TD (D=2)

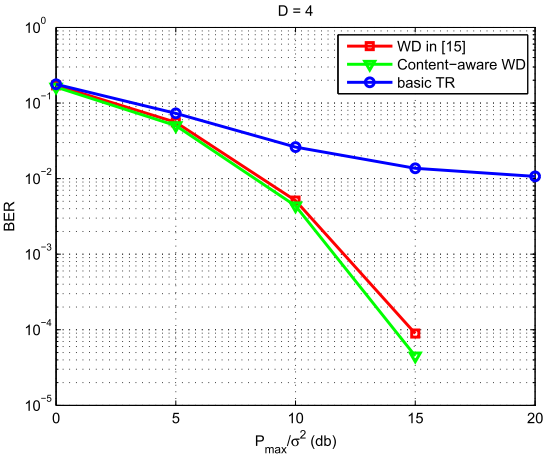

(b) The BER of the single RRH single TD (D=4)

Fig. 7. The BER Performance of Downlink Transmission in Single RRH Single TD Case.

Algorithm 3 Gradient Optimization Algorithm for Optimal Power Control in Uplink

Initialize $\beta(s,s) = \sqrt{\frac{P_{max}^{(ul)}}{\Sigma_q(s,s)}}$, $\forall s$
loop:
  Calculate $\nabla\beta$ according to (48) and (49)
  Set $n = 1$
  Update β^{proj} according to (50) and (51)
  if $MSE_{new} < MSE_{current}$
    $\beta = \beta^{proj}$
  else
    $n = n + 1$, go to step 5
until β converges or the maximum number of iterations is reached

In this subsection, we extend the LMMSE detector design and power control algorithm to the multiple RRH case.

In the multiple RRH case, we assume the M RRHs simultaneously observe the transmitted signal from the N TDs and forward the collected signal to the BBUs for processing. The BBUs collect the aggregation of the signal received by all the RRHs, which can be represented as

$$Z = R\beta Q + n, \tag{52}$$

where $Z = [Z_1^T, Z_2^T, \cdots Z_M^T]^T$, $R = [R_1^T, R_2^T, \cdots R_M^T]^T$, $n = [n_1^T, n_2^T, \cdots n_M^T]^T$.

The LMMSE detector design in (44) and the gradient power control algorithm can be readily extended to the multiple RRH case by replacing R_i by R and n_i by n, respectively.

V. Experimental Results

In this section, we will use some numerical results to illustrate the effectiveness of the proposed waveform design algorithms. We start with the experiment settings in which we collect the multipath channels. After that, we will show the BER and MSE performance of the proposed algorithms under various conditions.

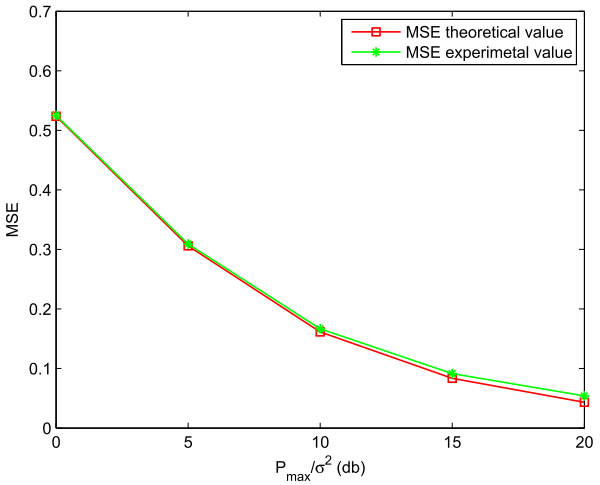

Fig. 8. The Theoretical and Experimental MSE of a Single TD.

A. Experiment Setting

We build a TR radio prototype to measure the multipath channel. A snapshot of the radio stations of our prototype is illustrated in Fig. 5, where a single antenna is attached to a small cart with RF board and computer installed on the cart. The tested signal bandwidth spans from 5.3375 GHz to 5.4625 GHz, centered at 5.4 GHz. An office room in the J. H. Kim Engineering Building at the University of Maryland is considered. As shown in Fig. 6a, the RRHs are placed at 6 locations across the room, while the TDs are placed in multiple locations in the small room marked with "A". The layout of room "A" and an example of the placement of the TDs are shown in Fig. 6b. In this experiment, we have 800 possible TD locations and 6 possible AP locations, from which 4800 independent multi-path channel measurements are obtained. In the following subsections, the performance of the proposed waveform design schemes are evaluated using the measured channels.

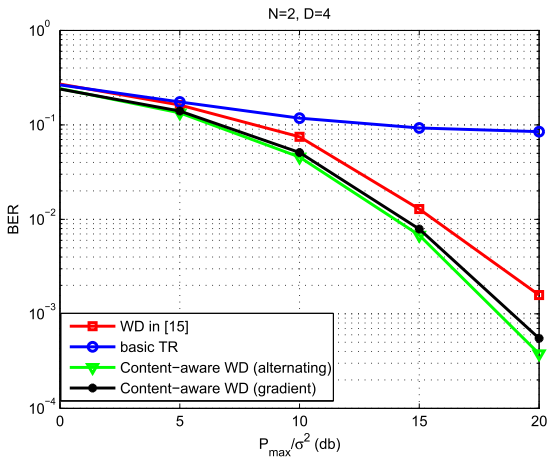

(a) The BER of the single RRH with two TDs (D=4)

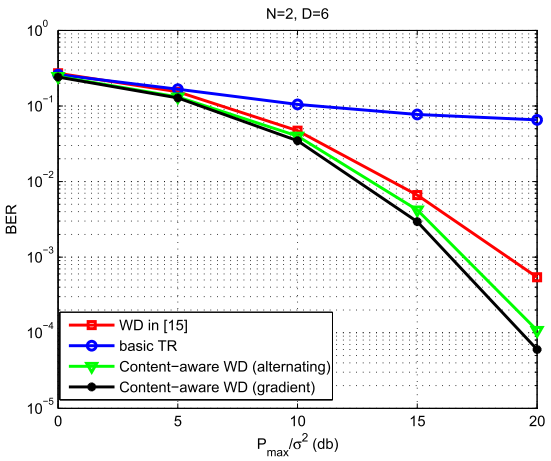

(b) The BER of the single RRH with two TDs (D=6)

Fig. 9. The BER Performance of Downlink Transmission in Single RRH Two TD Case.

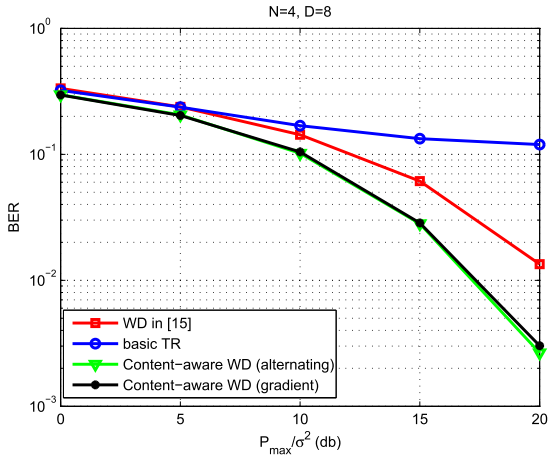

(a) The BER of the single RRH with Four TDs (D=8)

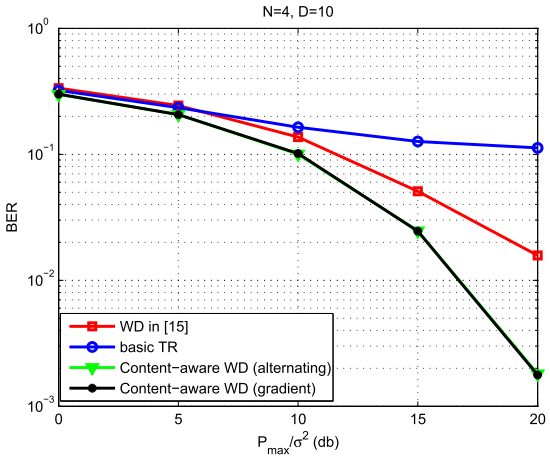

(b) The BER of the single RRH with Four TDs (D=10)

Fig. 10. The BER Performance of Downlink Transmission in Single RRH Four TD Case.

B. Single RRH Waveform Design

In this subsection, we show the numerical results obtained by using the single RRH waveform design algorithms proposed in section III and section IV.

In Fig. 7, we show the BER performance of the single RRH single TD waveform design algorithm. The curves labeled "Content-aware WD" stand for the performance of the algorithms proposed in this paper where the content information and the channel information are used in the waveform design. The curve labeled "WD" stands for the BER performance of the sum rate maximization waveform design algorithm proposed in [15]. In this algorithm, only the channel information is used to determine the waveform for downlink transmission. The curve labeled "TR" stands for the BER performance using basic TR waveforms used in [14]. As shown in the figures, as $\frac{P_{max}^{(dl)}}{\sigma^2}$ increases, the BER of the basic TR fails to go down since it is dominated by the interference. The BER decreases as $\frac{P_{max}^{(dl)}}{\sigma^2}$ increases for the algorithms proposed in this paper and in [15]. Moreover, the algorithm proposed in this paper always outperforms that in [15]. The reason is that the algorithms proposed in this paper utilizes extra content information to optimize the waveform. By comparing Fig. 7a and Fig. 7b, the performance gap between the algorithms in this paper and that in [15] shrinks when D increases, since the interference is less severe with larger D. Moreover, we show in Fig. 8 that the theoretical MSE calculated by (32) matches the theoretical values well.

Next, we evaluate the proposed design in the single RRH multiple TD setting. In Fig. 9 and Fig. 10, we show the BER performance of the proposed algorithm in the single AP and multiple TD settings. Similar to the single TD case, the BER of the basic TR goes down very slowly as $\frac{P_{max}^{(dl)}}{\sigma^2}$ increases due to the saturation of interference. The proposed algorithms always outperform that in [15] due to utilizing the extra content information. The performance gap is larger than the single TD case since the interference is more severe than the single TD case. Moreover, it is illustrated that the performance of the alternating algorithm is close to that of the gradient algorithm.

C. Multiple RRH Waveform Design

In Fig. 11, we show the BER performance of the algorithm in section III-B for the multiple RRH settings. The BER of the basic TR and zero-forcing waveforms goes down very slowly with the increase of $\frac{P_{max}^{(dl)}}{\sigma^2}$. On the other hand, in the proposed

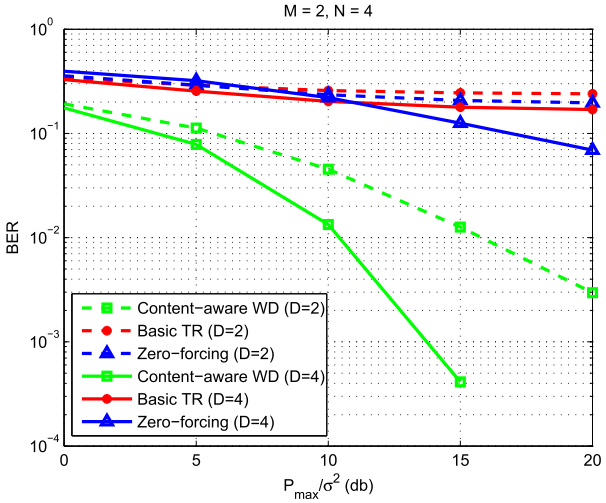

Fig. 11. The BER Performance of Downlink Transmission in a Multiple RRH Case.

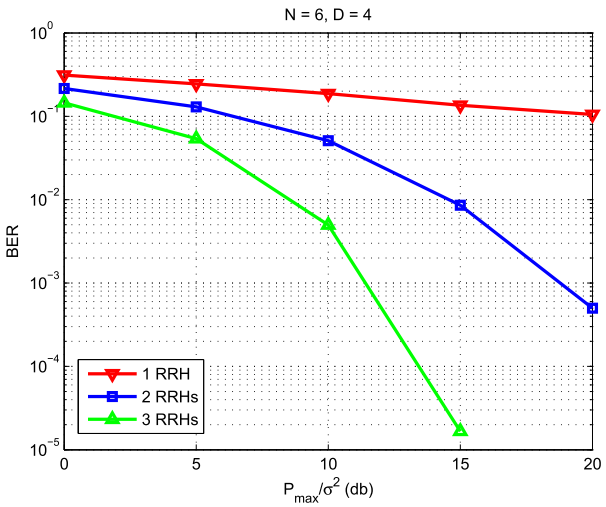

Fig. 12. The Improvement of BER by Adding RRHs in Downlink Transmission.

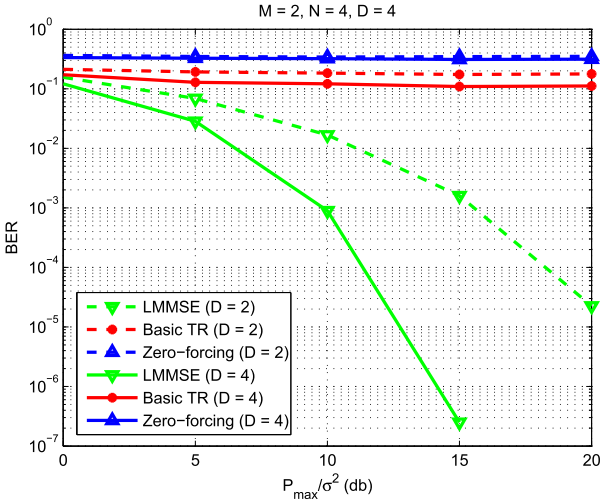

Fig. 13. The BER Performance of Uplink Transmission in a Multiple RRH Case.

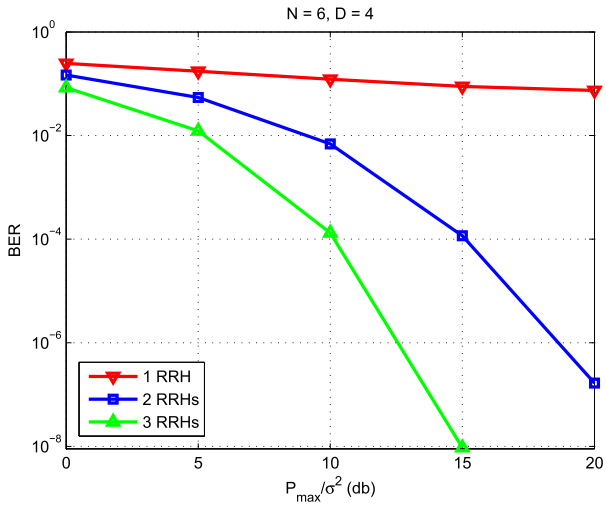

Fig. 14. The Improvement of BER by Adding RRHs in Uplink Transmission.

content-aware waveform design schemes, multiple RRHs work together to determine the transmitting power and waveform and thus achieve good interference management. As a result, the extra RRHs not only bring in more transmitting power, but also the additional degree of freedom that can be utilized to better focus the signal at the intended locations. As shown in Fig. 12, the average BER of the TDs decrease with more RRHs installed.

For the uplink case, we show the BER performance of the proposed algorithm in the multiple RRH setting. The curves labeled "LMMSE" stand for the performance of the proposed LMMSE estimator design, and the curves labeled "TR" stand for the performance of the basic TR waveforms in [13]. As shown in Fig. 13, the BER of the basic TR and zero-forcing waveforms goes down very slowly as $\frac{P_{max}^{(ul)}}{\sigma^2}$ increases. In particular, the BER of the zero-forcing waveform is high even in the high SNR region since the inter-user interference (IUI) dominates noise. On the other hand, by using the proposed algorithm, the observations from multiple RRHs are gathered and processed to detect the symbols transmitted by the TDs. Additional RRHs provide extra observations of the symbols transmitted by the TDs, which can be utilized to improve the accuracy of the detection. As shown in Fig. 14, the average BER of the TD decreases with the more RRHs installed.

VI. Conclusion

In this work, we studied the optimization on the downlink and uplink transmission in TR based C-RAN. The content/channel information and the computing power in the BBU pool is utilized to optimize the waveform design in the downlink and receiver design in the uplink. The asymmetric architecture of TR communication is preserved in the optimization and no change in the terminal device (TD) is needed. In this way, the performance of the TR based C-RAN can be improved while keeping the low cost of the TDs. We built a TR radio prototype to measure the wireless channel in the real-world environment, with which we illustrated that the proposed algorithms can significantly improve the downlink and uplink transmission reliability over basic TR waveforms and traditional waveform design schemes.

In the future, it might be interesting to investigate the efficient channel estimation scheme. As the number of

TDs scales up, the channel probing overhead might become a bottleneck for the system. It would be interesting to explore how to update the channel information from aggregate channel probing signal, so that more than one TDs can do the channel probing at the same time to save the channel probing overhead.

REFERENCES

[1] "C-RAN: The road towards green RAN," ChinaMobile, Beijing, China, White Paper, Oct. 2011.

[2] M. Webb, Z. Li, P. Bucknell, T. Moulsley, and S. Vadgama, "Future evolution in wireless network architectures: Towards a 'cloud of antennas,"' in *Proc. IEEE Veh. Technol. Conf. (VTC-Fall)*, Sep. 2012, pp. 1–5.

[3] C.-L. I, J. Huang, R. Duan, C. Cui, J. Jiang, and L. Lei, "Recent progress on C-RAN centralization and cloudification," *IEEE Access*, vol. 2, pp. 1030–1039, 2014.

[4] Y. D. Beyene, R. Jäntti, and K. Ruttik, "Cloud-RAN architecture for indoor DAS," *IEEE Access*, vol. 2, pp. 1205–1212, Oct. 2014.

[5] R. Wang, H. Hu, and X. Yang, "Potentials and challenges of C-RAN supporting multi-RATs toward 5G mobile networks," *IEEE Access*, vol. 2, pp. 1187–1195, 2014.

[6] Y. Zhou and W. Yu, "Optimized Backhaul compression for uplink cloud radio access network," *IEEE J. Sel. Areas Commun.*, vol. 32, no. 6, pp. 1295–1307, Jun. 2014.

[7] X. Rao and V. K. N. Lau, "Distributed fronthaul compression and joint signal recovery in cloud-RAN," *IEEE Trans. Signal Process.*, vol. 63, no. 4, pp. 1056–1065, Feb. 2015.

[8] S.-H. Park, O. Simeone, O. Sahin, and S. Shamai (Shitz), "Inter-cluster design of precoding and fronthaul compression for cloud radio access networks," *IEEE Wireless Commun. Lett.*, vol. 3, no. 4, pp. 369–372, Aug. 2014.

[9] B. Dai and W. Yu, "Sparse beamforming and user-centric clustering for downlink cloud radio access network," *IEEE Access*, vol. 2, pp. 1326–1339, Oct. 2014.

[10] O. Simeone *et al.*, "Downlink multicell processing with limitedbackhaul capacity," *EURASIP J. Adv. Signal Process.*, vol. 2009, no. 1, p. 840814, 2009.

[11] B. Wang, Y. Wu, F. Han, Y.-H. Yang, and K. J. R. Liu, "Green wireless communications: A time-reversal paradigm," *IEEE J. Sel. Areas Commun.*, vol. 29, no. 8, pp. 1698–1710, Sep. 2011.

[12] F. Han, Y. H. Yang, B. Wang, Y. Wu, and K. J. R. Liu, "Time-reversal division multiple access over multi-path channels," *IEEE Trans. Commun.*, vol. 60, no. 7, pp. 1953–1965, Jul. 2012.

[13] F. Han and K. J. R. Liu, "A multiuser TRDMA uplink system with 2D parallel interference cancellation," *IEEE Trans. Commun.*, vol. 62, no. 3, pp. 1011–1022, Mar. 2014.

[14] H. Ma, B. Wang, Y. Chen, and K. J. R. Liu, "Time-reversal tunneling effects for cloud radio access network," *IEEE Trans. Wireless Commun.*, vol. 15, no. 4, pp. 3030–3043, Apr. 2016.

[15] Y. H. Yang, B. Wang, W. S. Lin, and K. J. R. Liu, "Near-optimal waveform design for sum rate optimization in time-reversal multiuser downlink systems," *IEEE Trans. Wireless Commun.*, vol. 12, no. 1, pp. 346–357, Jan. 2013.

[16] E. Yoon, S. Y. Kim, and U. Yun, "A time-reversal-based transmission using predistortion for intersymbol interference alignment," *IEEE Trans. Commun.*, vol. 63, no. 2, pp. 455–465, Feb. 2015.

[17] S.-H. Park, O. Simeone, O. Sahin, and S. Shamai (Shitz), "Joint precoding and multivariate backhaul compression for the downlink of cloud radio access networks," *IEEE Trans. Signal Process.*, vol. 61, no. 22, pp. 5646–5658, Nov. 2013.

[18] Y. Shi, J. Zhang, and K. B. Letaief, "Group sparse beamforming for green cloud-RAN," *IEEE Trans. Wireless Commun.*, vol. 13, no. 5, pp. 2809–2823, May 2014.

[19] S. Luo, R. Zhang, and T. J. Lim, "Downlink and uplink energy minimization through user association and beamforming in C-RAN," *IEEE Trans. Wireless Commun.*, vol. 14, no. 1, pp. 494–508, Jan. 2015.

[20] A. Goldsmith, *Wireless Communications*. Cambridge, U.K.: Cambridge Univ. Press, 2005.

[21] S. Boyd and L. Vandenberghe, *Convex Optimization*. Cambridge, U.K.: Cambridge Univ. Press, 2004.

[22] B. Hajek, "An exploration of random processes for engineers," Dept. Elect. Comput. Eng., Univ. Illinois Urbana-Champaign, Urbana, IL, USA, Tech. Rep., 2009.

[23] K. B. Petersen *et al.*, "The matrix cookbook," *Tech. Univ. Denmark*, vol. 7, p. 15, Nov. 2008.

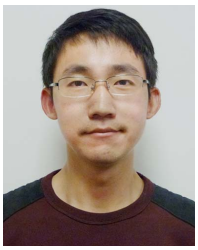

Hang Ma (M'17) received the B.S. degree in information engineering from Northwestern Polytechnical University, Xi'an, China, in 2010, and the Ph.D. degree in electrical engineering from the University of Maryland at College Park, College Park, USA, in 2016. His research interests include wireless communication and signal processing. He received the Honor of Outstanding Graduate of Northwestern Polytechnical University in 2010.

Beibei Wang (SM'15) received the B.S. degree (Hons.) in electrical engineering from the University of Science and Technology of China, Hefei, in 2004, and the Ph.D. degree in electrical engineering from the University of Maryland at College Park, in 2009. She was with the University of Maryland at College Park as a Research Associate from 2009 to 2010, and with Qualcomm Research and Development from 2010 to 2014. Since 2015, she has been with Origin Wireless Inc., where she is currently the Chief Scientist in wireless. She has co-authored *Cognitive Radio Networking and Security: A Game-Theoretic View* (Cambridge University Press, 2010). Her research interests include wireless communications and signal processing. She received the Graduate School Fellowship, the Future Faculty Fellowship, the Dean's Doctoral Research Award from the University of Maryland, and the Overview Paper Award from the IEEE Signal Processing Society in 2015.

Yan Chen (SM'14) received the bachelor's degree from the University of Science and Technology of China in 2004, the M.Phil. degree from The Hong Kong University of Science and Technology in 2007, and the Ph.D. degree from the University of Maryland at College Park, College Park, MD, USA, in 2011. He was with Origin Wireless Inc. as a Founding Principal Technologist. Since 2015, he has been a Full Professor with the University of Electronic Science and Technology of China. His research interests include multimedia, signal processing, game theory, and wireless communications.

Dr. Chen was a recipient of multiple honors and awards, including the Best Student Paper Award at the IEEE ICASSP in 2016, the Best Paper Award at the IEEE GLOBECOM in 2013, the Future Faculty Fellowship and Distinguished Dissertation Fellowship Honorable Mention from the Department of Electrical and Computer Engineering in 2010 and 2011, the Finalist of the Dean's Doctoral Research Award from the A. James Clark School of Engineering, University of Maryland at College Park, in 2011, and the Chinese Government Award for Outstanding Students Abroad in 2010.

K. J. Ray Liu (F'03) was a Distinguished Scholar-Teacher with the University of Maryland at College Park, College Park, in 2007, where he is currently a Christine Kim Eminent Professor of information technology. He leads the Maryland Signals and Information Group conducting research encompassing broad areas of information and communications technology, with recent focus on smart radios for smart life.

Dr. Liu is a fellow of the AAAS. He was a recipient of the 2016 IEEE Leon K. Kirchmayer Technical Field Award on Graduate Teaching and Mentoring, the IEEE Signal Processing Society 2014 Society Award, and the IEEE Signal Processing Society 2009 Technical Achievement Award. He was recognized by Thomson Reuters as a Highly Cited Researcher.

He is a member of the IEEE Board of Director as the Division IX Director. He was the President of the IEEE Signal Processing Society, where he has served as the Vice President—Publications and Board of Governor. He has also served as the Editor-in-Chief of the *IEEE Signal Processing Magazine*.

He received teaching and research recognitions from the A. James Clark School of Engineering, University of Maryland at College Park, including University-Level Invention of the Year Award, the College-Level Poole and Kent Senior Faculty Teaching Award, the Outstanding Faculty Research Award, and the Outstanding Faculty Service Award.